

A Combined $np_x - \bar{X}$ Control Chart to Monitor the Process Mean in a Two-Stage Sampling

Elvis S. Sampaio,^a Linda Lee Ho^{b,*†} and Pledson G. de Medeiros^c

This paper proposes a new combined $np_x - \bar{X}$ control chart for monitoring the mean of a process. A sample of size n is split into two sub-samples of sizes n_1 and $n_2 = n - n_1$, determined by an optimization search. The units of the first sub-sample are evaluated by attributes and plotted on an np_x control chart. If this chart signals an out-of-control condition, then values of the quality characteristic of interest are collected from the units of the second sub-sample, and the sample mean is calculated and plotted on an \bar{X} control chart. If both control charts signal, then the process is halted for adjustment. The possibility that all n items will not be inspected may lead to a reduction in both the cost and time spent on examining the sampled items. The performance of the proposed procedure is compared to that of two separate \bar{X} and np_x control charts. The proposed procedure exhibits superior performance to the \bar{X} control chart for a variety of sample sizes, n , and shifts, δ , of the target mean. The average time to signal (ATS) for the combined control chart was lower than that calculated for a single \bar{X} or np_x control chart, indicating that the combined control chart is an efficient tool for monitoring the process mean. Copyright © 2013 John Wiley & Sons, Ltd.

Keywords: quality control; monitoring the process mean; control chart; control chart \bar{X} ; np_x control chart; combined control chart

1. Introduction

Quality has become a decisive factor in choosing products and/or services. Offering high quality products and services is therefore one of the main objectives in a modern company. The search for more rigorous methods of quality control has led to the development of new statistical techniques applicable to the business and/or industrial environment. Nowadays, most companies employ some type of monitoring in the production process with the aim of improving their financial results and succeeding in a competitive market.

Improving the performance of control charts and devising new methods for their construction are an ongoing challenge for both researchers and users of statistical process control. The process mean can be shifted from its target value owing to a variety of variation sources, yielding instability in quality control assessments and preventing a company from reaching its goals. A variety of new control charts and monitoring strategies have therefore been developed in recent decades, including many contributions that combine two control charts for variables.

In the pioneering paper of Westgard *et al.*,¹ a combined Shewhart–CUSUM control chart was proposed to improve quality control in clinical chemistry. In this control chart, both sets of control limits were included in a single control chart. Figure 1 illustrates an example of the procedure proposed by Westgard *et al.*¹

Lucas and Crosier² obtained analytical expressions for the combined Shewhart–CUSUM control scheme and argued that Shewhart charts provide superior detection of large shifts, while smaller shifts are more readily detected using CUSUM control charts. Gibbons³ applied a combined Shewhart–CUSUM control chart to ground water monitoring. An optimization process for the combined Shewhart–CUSUM control chart was presented in Wu *et al.*,⁴ with the aim of improving the performance of the algorithm originally proposed by Lucas and Crosier.² Lucas and Saccucci⁵ suggested a combined Shewhart–EWMA control chart to improve the performance of the EWMA control chart on its own. Laungrungrong *et al.*⁶ employed a combined CUSUM–EWMA-type control chart in a study monitoring the strength of concrete. Another procedure for combining CUSUM and EWMA control charts was recently suggested by Abbas *et al.*⁷

Another control chart of interest is that proposed by Wu *et al.*,⁸ the np_x control chart. Using this chart, it is possible to monitor the process mean through attribute inspection. Following the determination of the optimum parameters, each sampled unit is classified as conforming or non-conforming. No value is assigned to the quality characteristic of interest, and the status of process assessment is simply based on the number of units classified as non-conforming. The good performance of the np_x control chart combined with its efficiency of implementation renders this control chart quite promising in the development of new monitoring methods.

Motivated by the contribution of Westgard *et al.*¹ and Wu *et al.*,⁸ a new combined $np_x - \bar{X}$ control chart is proposed to monitor the process mean in this paper. This control chart uses both attribute inspection (to draw the np_x control chart) and inspection by

^aUFRN, Natal, Brazil

^bUSP, São Paulo, Brazil

^cUFRN, Natal, Brazil

*Correspondence to: Linda Lee Ho, USP, São Paulo, Brazil.

†E-mail: lindalee@usp.br

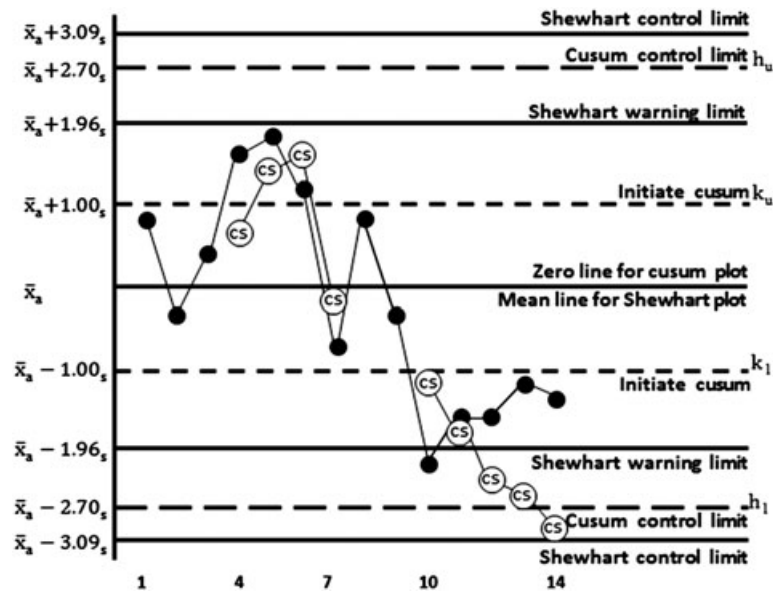


Figure 1. Combined Shewhart–CUSUM control chart proposed by Westgard et al. (1977)

variables (to draw the \bar{X} control chart). The sample is split into two sub-samples, determined by an optimization process. Items from the first sub-sample are evaluated based on attribute inspection, and a monitored statistic is used to draw the np_x control chart. If the np_x control chart signals an out-of-control condition, then values of the quality characteristic are taken from the second sub-sample and the sample mean is calculated and plotted on an \bar{X} control chart. If both charts signal, then the process is halted for adjustment. This procedure allows for an assessment based only on the inspection by attributes in some cases (omitting the inspection by variables), yielding a potential reduction in cost and time spent on the inspection.

In this article, it is assumed that the quality characteristic of interest follows a normal distribution with mean μ and variance σ^2 and that the observations of the process are independent and identically distributed. When the process is in-control, $\mu = \mu_0$ and $\sigma^2 = \sigma_0^2$. When the process is out-of-control, $\mu = \mu_1 = \mu_0 + \delta\sigma_0$ (and the standard deviation remains unchanged). Our objective is to detect unilateral shifts in the process mean; hereafter, all expressions are developed for the case $\delta > 0$.

The paper is organized as follows. In Section 2, the np_x control chart proposed by Wu *et al.*⁸ is described in detail. The new combined $np_x - \bar{X}$ control chart is the subject of Section 3, and a comparative performance study of this proposal is presented in Section 4. Some final considerations and suggestions for future research are discussed in Section 5.

2. The np_x control chart

The np_x control chart employs a dichotomous classification of items to monitor a process mean. Each item is classified as conforming or non-conforming, and the number of non-conforming items is used to assess the process.

Its implementation is similar to that of the traditional np control chart. An item is classified as non-conforming if the value of the quality characteristic falls in the interval $(w_U; \infty)$; otherwise, it is conforming Wu *et al.*⁸ referred w_U to as the warning limit, but in this paper, it is referred to as the upper discriminant limit (UDL).

Let D_{np_x} be the number of non-conforming items in a sample of n units. If $D_{np_x} > UCL_{np_x}$, where UCL_{np_x} is the upper control limit of the np_x control chart, then the process is judged to be out of control; otherwise, the process is in control.

In this paper, the $w_U = \mu_0 + k\sigma_0$ is determined by optimization to obtain a desirable level of parameter shift detection (see⁸). The user has the option to adjust the discriminant limit to attain a pre-specified level of parameter shift detection, (for example, in-control average length run (ARL_0)).

Other criteria can be used to determine the parameters UCL_{np_x} (an integer) and the discriminating limit, $w_U = \mu_0 + k\sigma_0$. For example, Wu *et al.*⁸ employed the Extra Quadratic Loss (EQL) criterion (see⁹ for further details), The parameters are chosen so as to minimize the EQL, with the requirement that must attain an in-control ATS (ATS_0) equal to τ .

Once w_U is determined, the probability p of one item being non-conforming is given by:

$$p = 1 - \Phi\left(\frac{w_U - (\mu_0 + \delta\sigma_0)}{\sigma_0}\right) \quad (1)$$

$$p = 1 - \Phi(k_w - \delta)$$

where $\Phi(\cdot)$ is the standard normal cumulative distribution function and k_w is the discriminant limit coefficient. The probability of type I error (known as risk α) is the probability of the control chart signaling when the process is in control; for the np_x control chart, this probability has the value:

$$\alpha = 1 - \sum_{d=0}^{UCL_{np_x}} \binom{n}{d} p_0^d (1 - p_0)^{n-d} \quad (2)$$

The risk β of type II error is the probability of the control chart failing to signal when the process is out of control; for np_x the control chart:

$$\beta = \sum_{d=0}^{UCL_{np_x}} \binom{n}{d} p_1^d (1 - p_1)^{n-d} \quad (3)$$

The values of p_0 and p_1 (the probability of the quality characteristic value falling outside the discriminant limits when the process is in control and out of control, respectively) are obtained from the expression (1), e.g., by setting $\delta = 0$ for p_0 .

In the traditional np control chart, an item is classified as conforming if the inspected item satisfies a set of requirements stated by the engineering team; otherwise, the item is non-conforming. Let F be the number of non-conforming items in a sample of n units. If $F > UCL$ where UCL is the upper control limit of the np control chart, then the process is judged to be out of control; otherwise, the process is in control.

Figure 2 shows a ring gage used in an attribute inspection (GO/NO GO) calibrated based on the discriminant limit, and Figure 3 shows an example of an np_x control chart. Note that the value of the statistic related to the eighth unit falls in the action region (beyond the out-of-control limits), indicating the presence of a particular cause (the process was judged to be out of control).

Comparative studies reveal that the np_x control chart is more efficient than the \bar{X} control chart if the inspection cost (per unit) of the first control chart is lower than that of the second. In this case, the sampling interval of the np_x control chart can be reduced or the sample size increased so that the np_x control chart displays a higher efficiency than its competitor.

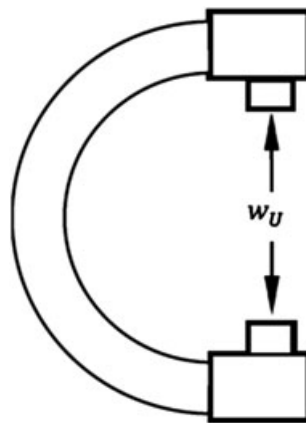


Figure 2. Ring gage

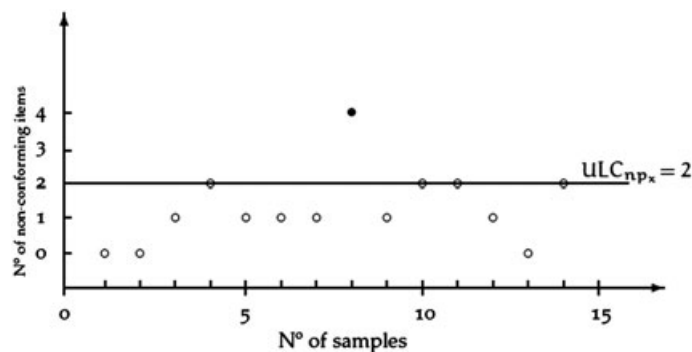


Figure 3. np_x chart control chart

3. The combined $np_x - \bar{X}$ control chart

In a production process monitored by a combined $np_x - \bar{X}$ control chart, two control charts of the np_x and \bar{X} types are constructed separately. The information from both charts is combined to assess the status of the process. A sample of size n is collected every h hours (the sampling interval), and this sample is split into two sub-samples of sizes n_1 and n_2 with $n_1 + n_2 = n$. The items in the sub-sample of size n_1 are evaluated by an attribute inspection. An item is classified as non-conforming if the value of the quality characteristic $\in (w_U; \infty]$. The number of non-conforming items in the first sub-sample of size n_1 , D_{np_x} , is used to draw the np_x control chart. If $D_{np_x} \leq UCL_{np_x}$, then the process is in control. In this case, the items in the second sub-sample (of size n_2) are reintegrated into the production process (or sent to the customers or the next production stage) and production proceeds normally. However, if $D_{np_x} > UCL_{np_x}$ the values of the quality characteristic are evaluated for the units in the second sub-sample, and the sample mean is calculated. If $\bar{X} \leq UCL_{\bar{X}}$, then the process is judged to be in control; otherwise, it is considered to be out of control. The halt for process adjustment occurs only if both control charts give a signal.

Note that according to this decision rule, all n items need not be inspected. The inspection by variables may not be realized, and the status of the process may be judged considering only the results of the inspection by attributes if the first sub-sample (of size n_1) indicates that the process is in control. Figure 4 shows an example in which all of the sampling statistics calculated from sub-samples of size n_1 do not exceed the upper control limit UCL_{np_x} . In this case, the inspection by variables is not realized in any of the sub-samples of size n_2 and no points are plotted in the \bar{X} control chart; the analysis consists only of the inspection by attributes and the combined control chart is reduced to an np_x control chart.

Figure 5 shows an example in which both control charts (\bar{X} and np_x) are employed. Observe that the inspection by variables is realized only in the 7th and 14th samples. In the first case, $\bar{X} \leq UCL_{\bar{X}}$, and the production continues, while in the second case, $\bar{X} > UCL_{\bar{X}}$, and the process is halted for adjustment.

Considering shift sizes $\delta > 0$ in the process mean, the probability of a process halt is given by:

$$P[(D_{np_x} > UCL_{np_x}) \cap (\bar{X} > UCL_{\bar{X}})] = P(D_{np_x} > UCL_{np_x})P(\bar{X} > UCL_{\bar{X}}) \tag{4}$$

with

$$P(D_{np_x} > UCL_{np_x}) = 1 - \sum_{d=0}^{UCL_{np_x}} \binom{n_1}{d} p^d (1-p)^{n_1-d} \tag{5}$$

$p = 1 - \Phi(k_w - \delta)$ and $k_w = \frac{w_U - \mu_0}{\sigma_0}$, where w_U is the UDL and $UCL_{\bar{X}} = \mu_0 + t_{\bar{X}} \frac{\sigma_0}{\sqrt{n_2}}$ is obtained by optimization.

A process may be incorrectly judged to be out of control (when it is in control: H_0); the probability of such a type I error (denoted by α_M) occurring for the proposed combined control chart is given by

$$\alpha_M = \alpha_{np_x} \alpha_{\bar{X}} \tag{6}$$

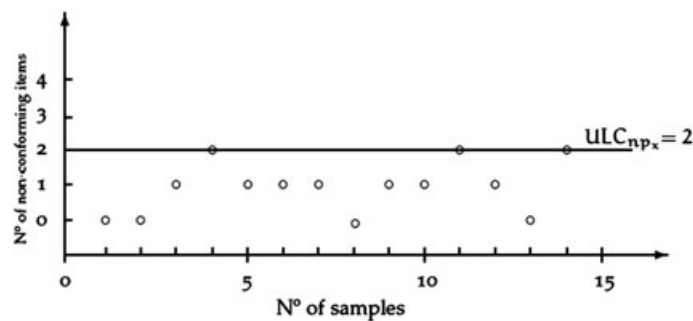


Figure 4. np_x control chart – a component of the combined control chart

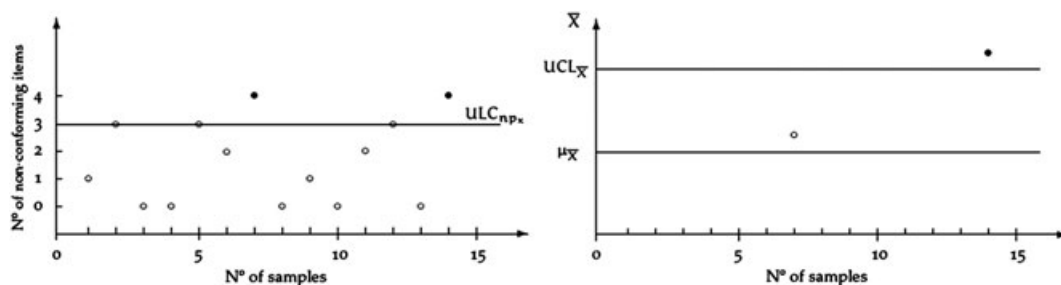


Figure 5. The combined $np_x - \bar{X}$ control chart

where

$$\alpha_{np_x} = P(D_{np_x} > UCL_{np_x} | p_0, n_1) \quad (7)$$

and

$$\alpha_{\bar{X}} = P(\bar{X} > UCL_{\bar{X}} | \mu_0, n_2) \quad (8)$$

For the process to be assessed as in control (H_0), two events can occur: $D_{np_x} \leq UCL_{np_x}$ or $D_{np_x} > UCL_{np_x} \cap \bar{X} \leq UCL_{\bar{X}}$. When the process is out of control (H_1), the probability of incorrectly judging it to be in control (type II error; denoted by β_M) for the combined control chart is:

$$\beta_M = 1 - P(D_{np_x} > UCL_{np_x} \cap \bar{X} > UCL_{\bar{X}} | H_1) = 1 - P(D_{np_x} > UCL_{np_x} | p_1, n_1) P(\bar{X} > UCL_{\bar{X}} | \mu_1 = \mu_0 + \delta \sigma_0, n_2) \quad (9)$$

The power of the combined control chart is given by:

$$Pd_M = 1 - \beta_M \quad (10)$$

The performance measure considered in this paper is the *ATS*. When the random time until a shift occurs follows a uniform distribution, the *ATS* is given by

$$ATS = \left(\frac{1}{1 - \beta_M} - 0.5 \right) h \quad (11)$$

and if the process is in control and $h = 1$, *ATS* is denoted by ARL_0 and given by (see⁹):

$$ARL_0 = \frac{1}{\alpha_M} \quad (12)$$

The sample sizes are constant for the \bar{X} and np_x control charts but not for the combined control chart. If the np_x control chart does not signal, then the sample size is n_1 ; otherwise, the sample size is $(n_1 + n_2)$. The average sample size (*ASS*) must therefore be considered in designing the combined control chart:

$$\begin{aligned} ASS &= E(\text{Sample size of the combined control chart}) \\ &= n_1 + n_2 \alpha_{np_x} \end{aligned} \quad (13)$$

As α_{np_x} in the equation (7) $\in [0;1]$, we have $ASS < (n_1 + n_2)$. In comparison with the \bar{X} control chart (with fixed sample size $n_{\bar{X}}$), the combined control chart may have sample size $n_1 + n_2 = n > n_{\bar{X}}$; however, its *ASS* can be tuned to match $n_{\bar{X}}$. The procedure may provide a lower *ATS* owing to the sample size without an expressive increase of the *ASS*. Other advantages of the combined control chart include a decreased time required for inspection (in general, inspection by attributes is faster than inspection by variables) and a lower average inspection cost (*AIC*),

$$AIC = n_1 c_{np_x} + n_2 \alpha_{np_x} c_{\bar{X}} \quad (14)$$

where c_{np_x} and $c_{\bar{X}}$ are the cost per unit in the np_x and \bar{X} control charts, respectively. The values of n_1 , n_2 and α_{np_x} that maximize the efficiency of the combined control chart are determined using an optimization process.

Several factors influence the performance of a control chart, including the sample size, control limits, and constants used in computing the control limits and error probabilities. There are uncountable combinations of such factors when designing a combined $np_x - \bar{X}$ control chart. Many of these combinations are inefficient, yielding higher *ATS* values. It is therefore necessary to search for an optimal combination of values.

Hence, the procedure employed to identify combinations that provide low *ATS* values but also satisfying a pre-determined in-control *ATS* value (ARL_0) such that could compete with the \bar{X} control charts is the following:

- The inputs for the optimization search: (i) the sample size for \bar{X} control charts, $n_{\bar{X}}$; (ii) sampling interval, h ; (iii) type error 1 of the combined control chart, α_M ; (iv) minimum value of the ARL_0 , τ ; (v) size of the shift in the process mean, δ ; and (vi) inspection costs per unit, c_{np_x} and $c_{\bar{X}}$.

Step 1: Considering the sample size for \bar{X} control charts, $n_{\bar{X}}$; calculate $ATS_{\bar{X}} = \left(\frac{1}{1 - \beta_{\bar{X}}} - 0.5 \right) h$; $\beta_{\bar{X}} = 1 - P(\bar{X} > UCL_{\bar{X}} | \mu_1 = \mu_0 + \delta \sigma_0, n_{\bar{X}})$ such that $ARL_0 = \tau$

Step 2:

For $n_2 = 1$ to $n_{\bar{X}} - 1$ by 1;

For $n_1 = 1$ to $n_{\bar{X}}$ by 1;

For $\alpha_{\bar{X}} = 0.005$ to 0.495 by 0.005 ;

For $UCL_{np_x} = 0$ to $n_1 - 1$ by 1;

use the sample size n_1 to obtain $\alpha_{np_x} = \frac{\alpha_M}{\alpha_{\bar{X}}}$;

```

Use the sample size  $n_2$  to obtain  $UCL_{\bar{X}}$ ;
Calculate  $ATS$  by the expression (11) such that in-control  $ATS$  must attend  $ARL_0 = \tau$ 
If  $ATS < ATS_{\bar{X}}$  then
Return  $n_1, n_2, UCL_{\bar{X}}, w_U, UCL_{np_x}, ATS; ASS; AIC; \alpha_{\bar{X}}; \alpha_{np_x}$ 
End
End
End
End
End

```

The outputs at the end of the optimization search are

- The sizes of the sub-samples (n_1 and n_2);
- The control limits ($UCL_{\bar{X}}$ and UCL_{np_x}) and UDL (w_U);
- The ASS , AIC , the ATS and values of α_{np_x} and $\alpha_{\bar{X}}$.

The optimization process provides many combinations with low ATS values that also satisfy the minimum $ARL_0 = \tau$ criterion. As the combined control chart is designed to compete with the \bar{X} control chart, the search for the second sub-sample size, n_2 , continues up to $n_{\bar{X}} - 1$, where $n_{\bar{X}}$ is the sample size of a single \bar{X} control chart. Similarly, the search for the first sub-sample size, n_1 goes up to $n_{\bar{X}}$ to maintain a comparable ASS for the combined control chart. It is important to point out that the search for the parameters of the np_x control chart optimizes the ATS and not the EQL as in Wu *et al.*⁸

The choice of parameters for the combined control chart will depend on economic and/or statistical criteria. The manager responsible for the process monitoring may choose a design to satisfy multiple criteria, such as lower inspection costs, lower ATS , and higher power of detection. Clearly, favorable results may not be obtained simultaneously for all criteria, and it is therefore necessary to prioritize the criteria used in the monitoring process. In each run, there are $n_{\bar{X}} \times (n_{\bar{X}} - 1)$ available combinations, and the set of parameters best matching his or her particular needs in quality monitoring (e.g. based on the ATS , inspection costs, or detection power) may be chosen by each user.

4. Comparative performance study

A comparative study was performed between the single control charts \bar{X} and np_x , and the combined $np_x - \bar{X}$ control chart. The following assumptions were adopted in this study:

- The quality characteristic follows a standard normal distribution when the process is in control;
- The sampling interval is $h = 1$;
- The sample size of the \bar{X} control chart satisfies $n_{\bar{X}} \in [3; 9]$;
- The sample size n for the combined control chart lies in the interval $3 \leq n_1 + n_2 = n \leq 17$
- There is no restriction on the sample size for the single np_x control chart, n_{np_x} ;
- The following values are considered for ARL_0 : $ARL_0 = 250; 370; 500$ and 700 .
- The following values are considered for the shift in the process mean: $\delta = 0.25; 0.5; 1$; and 2 .

A program was developed for the optimization process. Owing to the large number of possibilities, the following strategy was used to identify good competitors for the \bar{X} control chart. For a fixed sample size $n_{\bar{X}}$ and shift δ , combinations of parameters providing similar ATS values to those for the single \bar{X} control chart were selected for the single np_x and combined $np_x - \bar{X}$ control charts.

Preliminary analyses reveal that single np_x control charts and the combined $np_x - \bar{X}$ control chart are not efficient competitors when $n_{\bar{X}} = n = n_{np_x}$. Their performances improve when n and n_{np_x} , increase and in turn ASS increases. This may explain the inferior performance of single np_x control charts reported in previous studies, as a large increase in the sample size n_{np_x} may be costly. However, the search results lead us to a different conclusion. It is possible to construct configurations for the combined control chart with sample sizes $(n_1 + n_2) = n > n_{\bar{X}}$ but with ASS in the expression (13) $< n_{\bar{X}}$. Selecting configurations with lower ASS may be an efficient criterion for choosing good competitors (e.g., for high inspection cost processes). However, low ATS , high detection power, and/or low AIC as given in the expression (14) are alternative criteria to be considered when choosing good competitors.

Concerning the ATS , the performance of the combined control chart improves as the ASS increases. Therefore, the configuration yielding the superior performance when compared to the \bar{X} control chart is usually the one with the largest possible ASS value.

The following results are obtained for $ARL_0 = 370$. Similar behavior is observed for other values of ARL_0 , but is not described in detail for brevity. The combined control chart exhibits a configuration that provides 33% lower ATS for a shift of $\delta = 0.5$ ($ATS_{\bar{X}} = 9.505$ vs. $ATS_{np_x - \bar{X}} = 6.354$; $n_{\bar{X}} = 9$; $n_1 = 9$ and $n_2 = 8$); 28.8 % lower ATS for a shift of $\delta = 1$ ($ATS_{\bar{X}} = 2.204$ vs. $ATS_{np_x - \bar{X}} = 1.568$; $n_{\bar{X}} = 6$; $n_1 = 6$ and $n_2 = 5$) or a reduction of 25.4% for a shift of $\delta = 0.25$ ($ATS_{\bar{X}} = 46.926$ vs. $ATS_{np_x - \bar{X}} = 34.974$; $n_{\bar{X}} = 9$; $n_1 = 9$ and $n_2 = 8$). Inferior results are observed for a larger shift of $\delta = 2$; in this case, the superior configuration provides a reduction of only 11.5% in the ATS ($ATS_{\bar{X}} = 105.695$ vs. $ATS_{np_x - \bar{X}} = 93.363$; $n_{\bar{X}} = 3$; $n_1 = 3$ and $n_2 = 2$).

Several configurations of the combined control chart for $ARL_0=370$; shift $\delta = 0.25$ and sample size $n_{\bar{x}} \leq 6$ are shown in Table I. Configurations with $n_{\bar{x}} > 6$ are available but are not presented in the table. As shown in Table I, all configurations have ATS less than or equal to that for the single \bar{X} control chart, $ATS_{\bar{x}}$. For a fixed $n_{\bar{x}}$, there are many options. Note that the same configuration of the combined control chart can be effectively used in various situations. For example, the configuration $n_1 = 4, n_2 = 3$, yielding $ATS = 73.94$, is a good competitor for a single \bar{X} control chart with sample size $n_{\bar{x}} = 4$ or 5. Similarly, the configurations $(n_1 = 4, n_2 = 4)$ and $(n_1 = 5, n_2 = 4)$, which yield $ATS = 65.74$ and 61.68 , respectively, are good alternatives to a single \bar{X} control chart with sample size $n_{\bar{x}} = 5$ or 6.

Owing to the large number of configurations of the combined control chart that can compete with the single \bar{X} control chart, we choose one particular case to illustrate the details of the proposed procedure (see Table II). The characteristics of this case are as follows:

- $ARL_0 = 370$;
- Shifts of $\delta = 0.25; 0.50; 1.00$; and 2.00 .
- Sample sizes of $n_{\bar{x}} = 5$; $n_{np_x} = 5$ and 8 . Two sizes are considered to identify the relationship between the sample size and performance of the np_x control chart.
- From among the combined control chart possibilities with $n_1 < n_{\bar{x}}$ and $n_2 < n_{\bar{x}} - 1$, the configuration with $n_1 = 3$ and $n_2 = 4$ is chosen as it yields lower ATS and ASS .
- The cost of inspection is $c_{np_x} = 1.00$ for one item for the np_x control chart and $c_{\bar{x}} = 3.00$ for the \bar{X} control chart.

The following observations can be made from Table II:

- The ATS of the combined control chart is lower than that of the \bar{X} control chart for shifts of $\delta = 0.25, 0.5$, and 1 (see the top and bottom of column 2).
- The powers of the two control charts are very similar (top of column 3 for \bar{X} ; bottom of column 5 for the combined control chart).
- The AIC of the combined control chart is lower than that of the \bar{X} control chart ($\$4.622$ vs. $\$15.00$).
- The ASS of the combined control chart is ca. 29.1% lower than the sample size of the \bar{X} control chart. For a large shift ($\delta = 2$), both control charts display similar ATS ; however, other criteria, such as the ASS , recommend the combined control chart ($ASS = 3.721$ vs. 5 units).
- A sample of at least $n_{np_x} = 8$ is required for the np_x control chart to be competitive with the \bar{X} control chart (column 10 vs. column 2; all cases with $n_{np_x} = 5$ display higher ATS , as seen in column 6).
- The ATS values for the np_x control chart with sample size $n_{np_x} = 8$ are very close to those for the combined control chart. However, this increase in sample size also raises the AIC (73% higher when compared to the combined control chart).
- A remark on the optimal parameters for the combined control charts: although obtained through separate optimizations, some of the parameter values are the same for the three values of the shift. Some of the parameters, such as α_{np_x} and k_w , are related;

Table I. ATS of some competitors for \bar{X} control chart: $ARL_0 = 370$ and $\delta = 0.25$							
\bar{X}		np_x		Combined $np_x - \bar{X}$			
$n_{\bar{x}}$	$ATS_{\bar{x}}$	n_{np_x}	ATS_{np_x}	n_1	n_2	ASS	$ATS_{np_x - \bar{x}}$
3	105.7	5	93.95	2	2	2.12	101.76
				3	2	3.06	93.36
				4	3	2.32	87.51
4	88.4	6	84.86	2	2	4.05	83.92
				3	3	3.27	80.79
				4	3	4.16	73.94
				4	3	4.16	73.94
				3	4	3.54	70.88
5	75.75	8	70.27	5	3	5.10	68.69
				4	4	4.30	65.74
				5	4	5.21	61.68
				4	4	4.30	65.74
				3	5	3.90	62.90
				6	3	6.09	63.76
6	66.06	9	64.91	5	4	5.21	61.68
				4	5	4.54	58.93
				6	4	6.19	57.50
				5	5	5.45	55.70
				6	5	6.33	52.16
				4	4	4.30	65.74
				3	5	3.90	62.90
				6	3	6.09	63.76

Table II. Comparison of the performance of the control charts

(1)	(2)	(3)	(4)	(5)	(6)	(7)	(8)	(9)	(10)	(11)	(12)	(13)
\bar{X} control chart												
δ	$ATS_{\bar{X}}$	$Pd_{\bar{X}}$	$t_{\bar{X}}$	$UCL_{\bar{X}}$	ATS_{np_x}	Pd_{np_x}	k_w	UCL_{np_x}	ATS_{np_x}	Pd_{np_x}	k_w	UCL_{np_x}
0.25	75.75	0.013	2.78	1.24	93.96	0.010	1	3	70.27	0.012	0.92	4
0.5	20.30	0.048	2.78	1.24	29.26	0.031	1	3	18.11	0.041	0.92	4
1	2.917	0.293	2.78	1.24	4.89	0.156	1	3	2.57	0.219	0.92	4
2	0.548	0.955	2.78	1.24	0.95	0.705	1.5	2	0.53	0.810	0.92	3
$np_x - \bar{X}$ Combined Control Chart												
δ	$ATS_{np_x - \bar{X}}$	θ_1	θ_2	Pd_M	ASS	AIC	k_w	$t_{\bar{X}}$	UCL_{np_x}	$UCL_{\bar{X}}$	α_{np_x}	$\alpha_{\bar{X}}$
0.25	70.88	0.233	0.060	0.014	3.541	4.622	0.736	2.054	1	1.027	0.135	0.020
0.5	18.45	0.361	0.146	0.049	3.541	4.622	0.736	2.054	1	1.027	0.135	0.020
1	2.70	0.654	0.470	0.313	3.541	4.622	0.736	2.054	1	1.027	0.135	0.020
2	0.56	0.981	0.966	0.948	3.721	5.162	0.611	2.170	1	1.080	0.180	0.015
<p>$n_{\bar{X}}$: Sample size of a single \bar{X} chart n_{np_x}: Sample size of np_x chart Pd_M: Power of $np_x - \bar{X}$ chart Pd_{np_x}: Power of np_x control chart ATS: Average Time to Signal $t_{\bar{X}}$: Constant to obtain $UCL_{\bar{X}}$ $\alpha_{\bar{X}}$, α_{np_x}, α_M: Type I errors of \bar{X}, np_x and $np_x - \bar{X}$, respectively $\theta_1 = P(D_{np_x} > UCL_{np_x} H_1)$ $\theta_2 = P(\bar{X} > UCL_{\bar{X}} H_1)$</p>												
np_x control chart												
$n_{np_x} = 8$; C.I. = 5; $\alpha_{np_x} = 0.0027$												

however, the UCL_{np_x} parameter is independent of the others. Similar behavior was observed for other values of ARL_0 , and this may be an indication that the optimum configuration is more strongly influenced by the pair (n_1, n_2) than by the shift size, δ . When $n_1 = n_2 = 4$ (see Table III), the values of α_{np_x} are equal for $\delta = 0.25$ and $\delta = 0.5$.

The proposed combined control chart can be used in place of the single \bar{X} control chart to optimize the ATS , cost of inspection, and/or detection power. As stated previously, there are multiple alternative configurations for the combined control chart. The configuration of the combined control chart of Table II and a second configuration, which sample size of the first sub-sample is increased by one unit ($n_1 = 4$) (while holding the other assumptions of Table II fixed), are shown in Table III.

The configurations shown in Table III are also good options for monitoring the process mean. Comparing Tables II and III, observe that all performance indicators are improved by the use of the combined control chart. The only control strategy that is not outperformed by the combined control chart is the np_x control chart with $n_{np_x} = 8$ when the shift is large ($\delta = 2$) (see the top of column 11 in Table II). The power of the combined control chart is also higher across the board in Table III. For example, for $\delta = 0.5$, the power is ca. 22.9% higher than for the \bar{X} control chart (top of column 3 in Table II). Note the considerable improvement in performance in the configuration of Table III without any significant increase in the ASS or inspection cost.

The enhancement in performance of the combined control chart over a single \bar{X} control chart is similar for other values of ARL_0 . For $ARL_0 = 250$, reductions of 24%, 31%, 26%, and 11% in ATS were observed for shifts of $\delta = 0.25, 0.5, 1$, and 2 , respectively. The best performance was observed for $ARL_0 = 700$; in this case, the ATS reductions were 27.7%, 36.2%, 32.6%, and 13.2% for $\delta = 0.25, 0.5, 1$, and 2 , respectively. The behavior with $ARL_0 = 500$ was very similar to that observed with $ARL_0 = 370$. It is therefore possible in general to find a configuration of the combined control chart exhibiting improved performance over a single \bar{X} control chart.

The ratios of the ATS for a single \bar{X} control chart to that for a combined control chart with $n_1 = n_{\bar{x}}$ and $n_2 = n_{\bar{x}} - 1$ (providing the optimal ATS results) are shown in Table IV. This configuration of the sub-samples generally results in $n_{\bar{x}} \leq ASS \leq n_{\bar{x}} + 1$ corresponding to a feasible number of inspections. Other combinations are therefore expected to provide inferior performance compared to that shown in Table IV. For example, the ratio of ATS is $\in [1.00; 1.12]$ for other configurations with

Table III. Comparison of two configurations of the combined control chart

	Size of the shift δ							
	0.25		0.50		1		2	
	$n_1 = 4$	$n_1 = 3$	$n_1 = 4$	$n_1 = 3$	$n_1 = 4$	$n_1 = 3$	$n_1 = 4$	$n_1 = 3$
ATS	65.75	70.88	16.43	18.45	2.37	2.70	0.54	0.56
θ_1	0.159	0.233	0.287	0.361	0.647	0.146	0.983	0.981
θ_2	0.095	0.060	0.226	0.146	0.598	0.479	0.963	0.966
Pd_M	0.015	0.014	0.059	0.049	0.348	0.313	0.963	0.948
ASS	4.309	3.541	4.309	3.541	4.360	3.541	4.432	3.721
AIC	4.924	4.622	4.924	4.622	5.080	4.622	5.296	5.162
k_w	0.550	0.736	0.550	0.736	0.501	0.736	1.040	0.611
$t_{\bar{x}}$	1.810	2.054	1.810	2.054	1.880	2.054	1.960	2.170
UCL_{np_x}	2	1	2	1	2	1	1	1
$UCL_{\bar{x}}$	0.900	1.027	0.900	1.027	0.940	1.027	0.980	1.080
α_{np_x}	0.077	0.135	0.077	0.135	0.090	0.135	0.108	0.180
$\alpha_{\bar{x}}$	0.035	0.020	0.035	0.020	0.030	0.020	0.025	0.015

Table IV. Ratios of ATS (\bar{X} control chart versus $np_x - \bar{X}$ combined control chart)

$n_{\bar{x}}$	$ARL_0 = 250$				$ARL_0 = 700$			
	Size of shifts δ				Size of shifts δ			
	0.25	0.5	1	2	0.25	0.5	1	2
3	1.12	1.20	1.26	1.10	1.15	1.25	1.34	1.17
4	1.15	1.29	1.33	1.06	1.21	1.36	1.43	1.11
5	1.21	1.33	1.35	1.03	1.25	1.41	1.46	1.06
6	1.24	1.38	1.36	1.01	1.29	1.47	1.48	1.02
7	1.27	1.40	1.35	1.00	1.32	1.50	1.47	1.01
8	1.29	1.43	1.32	1.00	1.35	1.54	1.45	1.00
9	1.31	1.45	1.30	1.00	1.38	1.56	1.43	1.00

$n_{\bar{x}} = 3$ and $ARL_0 = 250$. Observe that this ratio approaches one as the shift increases, indicating that the combined control chart provides superior performance for small shifts in the process mean. Similar behavior is observed for other values of ARL_0 , and these results are omitted for brevity.

It is important to highlight the type I error, the probability α_M used to obtain ARL_0 . This probability must be derived from both control charts comprising the combined control chart. Observe that the type I error in each individual component gives a high proportion of false alarms ($\alpha_{\bar{x}}$ or α_{np_x} ; see the bottom of columns 12 and 13 in Table II and the bottom of columns 6 and 7 in Table III), while α_M reaches desirable levels.

Finally, as the parameter setting may not be unique, some guidelines are presented to help the practitioners to choose best configurations among many alternative optimal parameters. Applying the procedure presented in Section 3, one has a set of the optimal parameters that provide low ATS values while also satisfying a pre-determined in-control ATS value (ARL_0) such that could compete with the \bar{X} control charts (so all configurations presented in Table I are qualified candidates). The practitioners should have listed which aspects are most important to consider in their criteria to make a choice. If the time to signal is the most relevant, then the configurations $(n_1 = 3; n_2 = 2); (n_1 = 4; n_2 = 3); (n_1 = 5; n_2 = 4); (n_1 = 6; n_2 = 5)$ can be used to compete with the \bar{X} control charts, respectively, for $n_{\bar{x}} = 3; 4; 5; 6$. However, if the practitioners consider only the cost spent in the inspection as the most important, the best configurations are other ones. Table V presents average inspect costs (AIC) of the candidates of Table I. They are obtained considering an extreme situation when cost for an attribute inspection is equal to the cost for inspection by variables (both equal to \$5.00). In this case, the best configurations are $(n_1 = 2; n_2 = 2); (n_1 = 2; n_2 = 3); (n_1 = 3; n_2 = 4); (n_1 = 3; n_2 = 5)$, respectively, for $n_{\bar{x}} = 3; 4; 5; 6$. The users may use another criterion, as for example a weighted average of AIC and ATS to choose good configurations.

5. Final considerations

In this paper, a new control chart was proposed to monitor the mean of a process. The proposed procedure consists of two sampling stages and combines two control charts: the np_x and \bar{X} control charts. The units of the first sample of size n_1 are evaluated by an attribute inspection, and the monitored statistic is used to draw the np_x control chart. If this chart signals, then the units of a second sample of size n_2 are evaluated, and the sample mean is used to draw the \bar{X} control chart. If the \bar{X} chart also signals, then the process is halted for adjustment.

The parameters for the combined control chart are chosen using an optimization process. The performances of the combined, single np_x and single \bar{X} control charts are compared for shift sizes of $\delta = 0.25; 0.5; 1$ and 2 and for $ARL_0 = 250; 370; 500$ and 700 . Owing to the large number of possibilities yielding performances superior to that of the single \bar{X} control chart, some guidelines are presented to help the practitioners to choose best configurations among many alternative optimal parameters.

A specific configuration is selected for the comparative study, with $n_1 = n_{\bar{x}}$ and $n_2 = n_{\bar{x}} - 1$, as this configuration provides favorable ATS values and $n_{\bar{x}} \leq ASS \leq n_{\bar{x}} + 1$.

Table V. AIC of some competitors for \bar{X} control chart: $ARL_0 = 370$ and $\delta = 0.25$							
\bar{X}		np_x		Combined $np_x - \bar{X}$			
$n_{\bar{x}}$	$AIC_{\bar{X}}$	n_{np_x}	AIC_{np_x}	n_1	n_2	ASS	$AIC_{np_x - \bar{X}}$
3	15	5	25	2	2	2.12	10.60
				3	2	3.06	18.40
				2	3	2.32	11.62
4	20	6	30	4	2	4.05	20.27
				3	3	3.27	16.35
				4	3	4.16	20.81
				4	3	4.16	20.81
				3	4	3.54	17.70
5	25	8	40	5	3	5.10	25.54
				4	4	4.30	21.54
				5	4	5.21	26.08
				4	4	4.30	21.54
				3	5	3.90	16.92
				6	3	6.09	30.45
6	30	9	45	5	4	5.21	26.08
				4	5	4.54	27.70
				6	4	6.19	30.98
				5	5	5.45	27.25
				6	5	6.33	31.70
				4	5	4.54	27.70
				5	4	5.21	26.08

The proposed control chart exhibits good performance in monitoring small to medium shifts. For shifts as large as $\delta = 2$, its performance is very similar to that of a single \bar{X} control chart.

The current paper is concerned with the detection of unilateral shifts in the process mean. However the proposed strategy can easily be adapted for the detection of bilateral shifts with relatively few adjustments. A natural extension of the control strategy proposed in this paper is to apply the method to multivariate process control.

Acknowledgements

The authors would like to thank CNPq-Brazil and Capes for the partial financial support and also acknowledge the anonymous referee for the suggestions.

References

1. Westgard JO, Groth T, Aronsson T, De Verdier C. Combined Shewhart-Cusum Control Chart For Improved Quality Control In Clinical Chemistry. *Clinical Chemistry* 1977; **23**(10):1881–1887.
2. Lucas JM, Crosier RB. Fast Initial Response For Cusum Quality-Control Schemes: Give Your Cusum a Head Start. *Technometrics* 1982; **24**(3):199–205.
3. Gibbons, RD. Use Of Combined Shewhart-Cusum Control Charts for Ground Water Monitoring Applications. *Ground Water* 1999; **5**:682–691.
4. Wu Z, Yang M, Jiang W, Khoo MBC. Optimization Designs of the Combined Shewhart-Cusum Control Charts. *Computational Statistics and Data Analysis* 2008; **53**:496–506.
5. Lucas JM, Saccucci MS. Weighted Moving Average Control Schemes: Properties and Enhancements. *Technometrics* 1990; **32**(1):1–12.
6. Laungrungrong B, Mobasher B, Montgomery D, Borrer CM. Hybrid Control Charts for Active Control and Monitoring of Concrete Strength. *Journal of Materials in Civil Engineering* 2010; **22**(1):77–87.
7. Abbas N, Riaz M, Does RJMM. Mixed Exponentially Weighted Moving Average-Cumulative Sum Charts for Process Monitoring. *Quality And Reliability Engineering International* 2012; (Article First Published Online: 29 Feb 2012 Doi: 10.1002/Qre.1385)
8. Wu Z, Khoo MBC, Shu L, Jiang W. An Np Control Chart for Monitoring the Mean of a Variable Based on an Attribute Inspection. *International Journal of Production Economics* 2009; **121**:141–147.
9. Reynolds Jr MR, Stoumbos ZG. Control Charts and the Efficient Allocation of Sampling Resources. *Technometrics* 2004; **46**:200–214.

Authors' biographies

Elvis S Sampaio received his MSc (2012) from Universidade do Rio Grande do Norte (Brazil). His main interest is statistical process control.

Linda Lee Ho received her PhD. (1995) from Universidade de São Paulo (Brazil). Since 1990 she has been professor at Departamento de Engenharia de Produção de Escola Politécnica of the same university. Her major research interests are statistical process control and design of experiments.

Pledson G de Medeiros received his Ph.D. (2003) from Universidade de São Paulo (Brazil). He is currently Associate Professor at the Federal University of Rio Grande do Norte. His major researchs interest is statistical process control.